Simplifying the simulation of local Hamiltonian dynamics

Ayaka Usui [1,2,*] Anna Sanpera,[3,4,†] and María García Díaz [5,‡]

[1]*Departament de Física Quàntica i Astrofísica, Institut de Ciències del Cosmos (ICCUB), Facultat de Física, Universitat de Barcelona, Martí i Franqués, 1, E08028 Barcelona, Spain*

[2]*Grup d'Òptica, Departament de Física, Universitat Autònoma de Barcelona, 08193 Bellaterra, Spain*

[3]*Física Teòrica: Informació i Fenòmens Quàntics, Departament de Física, Universitat Autònoma de Barcelona, 08193 Bellaterra, Spain*

[4]*ICREA, Pg. Lluís Companys 23, 08010 Barcelona, Spain*

[5]*Departamento de Matemática Aplicada a la Ingeniería Industrial, Universidad Politécnica de Madrid, 28006 Madrid, Spain*

(Received 7 November 2023; accepted 18 April 2024; published 4 June 2024)

Local Hamiltonians H_k describe nontrivial k-body interactions in quantum many-body systems. Here, we address the dynamical simulatability of a k-local Hamiltonian by a simpler one $H_{k'}$ with $k' < k$, under the realistic constraint that both Hamiltonians act on the same Hilbert space. When it comes to exact simulation, we build upon known methods to derive examples of H_k and $H_{k'}$ that simulate the same physics. We also address the most realistic case of approximate simulation. There, we upper-bound the error up to which a Hamiltonian can simulate another one, regardless of their internal structure, and show an example suggesting that the accuracy of a $(k' = 2)$-local Hamiltonian to simulate H_k with $k > 2$ increases with k. Finally, we propose a method to search for the k'-local Hamiltonian that simulates, with the highest possible precision, the short time dynamics of a given H_k Hamiltonian.

DOI: 10.1103/PhysRevResearch.6.023243

I. INTRODUCTION

A quantum simulator (QS) aims at replicating the physics of another quantum system, the properties of which are extremely difficult to obtain [1]. Currently, most of the existing QS are analog, i.e., naturally realize the physics of the target system and mimic its properties. Moreover, they are highly specialized experimental platforms acting as single-purpose simulators, and all of them, independently of the physical architecture on which they are implemented, face some problems regarding applicability, scalability, complexity, state preparation, control, and measurement (see e.g., [2] and references therein). It is desirable and expected that in the forthcoming years, some analog QSs will evolve into highly flexible devices, and also digital QSs, i.e., circuit-based quantum computers, will be further developed. Both classes of QS will be capable of simulating different quantum systems, preparing specific quantum states on demand, or analyzing their dynamics. This also includes the current NISQ (Noise Intermediate Scalable Quantum) platforms such as superconducting qubits, cold atoms and ions, Rydberg atoms, etc. Such versatility demands the development of theoretical frameworks capable of assessing the possibilities and applications of QS in areas as diverse as condensed-matter, high-energy physics, quantum chemistry, quantum gravity, out-of-equilibrium quantum physics or others [2–6].

As reflected in the literature [4,7–10], there are different approaches to defining the general conditions that a QS should fulfill. Those are obviously linked to the particular requirements needed to achieve a given goal, which in turn can also depend on the specific platform on which the QS will be implemented.

On the one hand, there is the strongest notion of a "universal" QS: a quantum many-body system simulates another one if it is able to reproduce its entire physics, i.e., it replicates its eigenstates, full energy spectrum, time evolution, any local noise process, correlation functions, observables, and thermal properties. This is the path developed in a series of very remarkable papers [9,11–13] based on a perturbative approach (perturbative gadgets) proposed initially in [14]. Within this approach the authors proved that the physics of any quantum many-body system can be replicated by certain 2-local spin-lattice models. The latter should be embedded in a Hilbert space significantly larger than that of the system to be replicated. Even a simple translationally invariant spin chain in 1D turns out to be a *universal simulator* in the above sense [11]. Nevertheless, such an approach is not constructive and comes with the additional challenge of requiring a scale-up of the simulation platforms, either by increasing the local dimension of the many-body system acting as a simulator and/or demanding an exquisite control over the interactions, which cannot be implemented in current and/or near future

*ayaka.usui@uab.cat
†anna.sanpera@uab.cat
‡maria.garcia.diaz@upm.es

experiments. On the other hand, there are less demanding definitions of quantum simulation where the spell is put on simulating either the ground-state or the low-energy physics of a complex quantum many-body system or some restricted dynamics. Simulating the dynamics of many-body quantum systems is, in general, a very difficult task for a classical or even for a NISQ device. Some advances have been recently proposed in this direction. For example, the purpose of [8,15] is to find a QS, whose time evolution in a restricted subspace is identical to that of the target system. In [8], the goal is to increase the locality of the QS, and this is achieved by requiring an additional qubit on each k-body interaction. On the contrary, in [15], the dimension of the QS does not increase, but the locality of both Hamiltonians remains the same.

Our paper is aligned with the latter ones in that our interest is placed on simulating dynamics of a target k-local Hamiltonian using a k'-local Hamiltonian for $k' < k$, i.e., the simulator is more local than the target. We do not attempt to embed the QS in a Hilbert space larger than the one associated to the target Hamiltonian, given that adding qudits to an experimental platform remains a challenging task. Also, for simplicity, we restrict our Hamiltonians to be 1D. Our purpose is to investigate the simulation of quantum many-body dynamics with the following two aims: simplifying complexity while maintaining the local dimension of the parties and the total dimension of the Hamiltonian.

Our paper is organized as follows. After presenting some preliminary concepts, in Sec. III we focus on exact dynamics and show, by means of an example, how some dynamics of a target Hamiltonian H_T can be replicated exactly by a simulator H_{QS} with simplified interactions in the same Hilbert space. In this example both Hamiltonians commute, which is a quite exceptional condition. Nevertheless, when considering noncommuting Hamiltonians, i.e., $[H_T, H_{QS}] \neq 0$, it is still possible to reproduce some dynamical behavior on a certain energy subspace, providing that both Hamiltonians have some eigenstates in common. It is hard to search for such shared subspaces by diagonalizing large Hamiltonians, and thus we present a generic upper bound to the dimension of such subspaces. In Sec. IV, we consider the most realistic case of nonexact simulation. There, we provide an upper bound to the error up to which any Hamiltonian is able to simulate another one, irrespectively of their structure. In an attempt to understand how such upper bound depends on locality, we present an interesting case suggesting that the precision with which a certain 2-local QS simulates a broad family of target Hamiltonians increase while the locality of the target Hamiltonian decreases. This suggests that, at least in certain cases and in reduced dimensionalities, a k-local H_T could be simulated better by a 2-local H_{QS} as k increases, or in other words, the less local H_T is. Finally, after showing that the worst-case error of simulation decreases when considering short times as expected, we develop a simple algorithm to find the k'-local Hamiltonian that best simulates a given k-local Hamiltonian in the short-time regime.

II. PRELIMINARY CONCEPTS

Most of quantum many-body systems are described by local Hamiltonians, and a vast majority of them only involve 2-body interactions. However, there are well-known examples of relevant many-body Hamiltonians (lattice gauge theories, Kitaev topological models, etc.) where interactions are not 2-body and whose properties are very difficult to analyze. To fix concepts, we denote by $\mathcal{H}_N$ an N-dimensional Hilbert space and by $\mathcal{B}(\mathcal{H}_N)$ the set of its bounded operators. An n-qudit *k-local* Hamiltonian $H \in \mathcal{B}(\mathcal{H}_{d^n})$ is of the form $H = \sum_{i=1}^{M} h_i$, where h_i is a Hamiltonian acting nontrivially on at most k parties, and M is some positive integer. An n-qudit k-local Hamiltonian with $k = n$ is dubbed *nonlocal*. Furthermore, a k-local Hamiltonian is said to be *more local* than a k'-local Hamiltonian if $k < k'$. Note that k locality does not necessarily imply interaction among k next-neighboring objects, and that there is no restriction on spatial locality.

We denote by $H_T \in \mathcal{B}(\mathcal{H}_{N_T})$ the Hamiltonian describing the target quantum system, the time evolution of which is to be replicated. The system achieving such quantum simulation will, in turn, be described by a Hamiltonian $H_{QS} \in \mathcal{B}(\mathcal{H}_{N_{QS}})$. As discussed previously, here we impose that $N := N_T = N_{QS}$. We hereby introduce our precise definition of simulation ($\hbar = 1$ is set throughout the whole paper):

Definition 1. A Hamiltonian H_{QS} ϵ-simulates a target Hamiltonian H_T at state $|\psi\rangle$ and time t if

$$|\langle\psi|e^{itH_{QS}}e^{-itH_T}|\psi\rangle| \geqslant 1-\epsilon, \tag{1}$$

with $\epsilon \in (0, 1]$.

Notice that $\epsilon = 0$ implies that the fidelity is 1, meaning that H_{QS} simulates H_T exactly in a subspace $\mathcal{S} \subset \mathcal{H}_N$, where $|\psi\rangle$ belongs. Maximizing ϵ over initial states and times informs us about the minimal performance of a given H_{QS} at simulating a certain H_T. The following definition can be put forward.

Definition 2. The worst-case fidelity of simulation for given Hamiltonians H_{QS} and H_T is defined as

$$\min_{\psi,t} |\langle\psi|e^{itH_{QS}}e^{-itH_T}|\psi\rangle|. \tag{2}$$

III. EXACT SIMULATION

In this section we address the scenario of error-free simulation, i.e., when $\epsilon = 0$. We illustrate this scenario by showing examples of both commuting and noncommuting Hamiltonians, which generate the same dynamics despite their different locality.

A. Commuting Hamiltonians

Using the Baker-Campbell-Hausdorff (BCH) formula, one can write condition (1) as

$$|\langle\psi|e^{i\tilde{H}(t)}|\psi\rangle| = 1, \tag{3}$$

with $\tilde{H}(t) := t(H_{QS} - H_T) + \frac{it^2}{2}[H_{QS}, -H_T] + \cdots$, where the remaining terms involve higher-order commutators of H_{QS} and H_T. In order for the BCH series to converge absolutely in this case, note that H_{QS} and H_T must fulfill $\|H_{QS}\| + \|H_T\| < \pi/t$, for a given submultiplicative norm $\|\cdot\|$ [16,17]. Given a target Hamiltonian H_T, one can now ask for which H_{QS}, initial states $|\psi\rangle$ and times t, condition (3) is fulfilled. An answer was provided in [15], which we briefly sketch in what follows: consider H_{QS} such that $[H_{QS}, H_T] = 0$,

and define the connector $h := H_{QS} - H_T$. Now write the initial state in the basis $\{|\phi_j\rangle\}_j^N$ which diagonalizes h: $|\psi\rangle = \sum_{j=1}^N a_j|\phi_j\rangle$, where $a_j = \langle\phi_j|\psi\rangle$. Then condition (3) becomes $|\sum_{j=1}^N |a_j|^2 e^{i\lambda_j t}| = 1$, with λ_j the jth eigenvalue of h. If $a_j \neq 0$ for each $j \in [1, N]$, the previous condition holds if h is fully degenerate, implying that H_{QS} is simply H_T plus some multiple of the identity. In order to avoid this trivial scenario, we naturally require that $|\psi\rangle$ is only spanned by the degenerate eigenvectors of h, i.e., $a_j \neq 0$ for all j such that $|\phi_j\rangle$ is degenerate and $a_j = 0$ otherwise. All in all, any Hamiltonian H_{QS} that commutes with a target Hamiltonian H_T is able to simulate H_T exactly at any time t and at any initial state spanned by the degenerate eigenvectors of the corresponding connector. Note that e^{ith} converges absolutely, as does the exponential of any square matrix.

As an example of this approach, in [15] it was shown that an infinite-range-interaction (2-body all with all interactions) Hamiltonian can be simulated using a nearest-neighbor-interaction model with a staggered field. Notice that, in this case, both H_T and H_{QS} are 2-local Hamiltonians. Here, we demonstrate, by means of a toy model, that the same approach can be employed to find instances of Hamiltonians *with different localities* that also lead to the same dynamics.

As an ideal terrain to understand such dynamics, let us consider a simple case in which only 4-qubits are involved. Let the 3-local Hamiltonian

$$H_T = \sum_{j=1}^{4} \left(J_3 \sigma_z^j \sigma_z^{j+1} \sigma_z^{j+2} + h_x \sigma_x^j\right), \tag{4}$$

describing a one-dimensional system, be our target Hamiltonian. By engineering the (2-local) Heisenberg XYZ model

$$H_{QS} = \sum_{j=1}^{4} \left(J_x \sigma_x^j \sigma_x^{j+1} + J_y \sigma_y^j \sigma_y^{j+1} + J_z \sigma_z^j \sigma_z^{j+1}\right) \tag{5}$$

we are able to obtain a QS Hamiltonian, which commutes with H_T and such that the corresponding connector has some degeneracy. Notice that $\|[H_T, H_{QS}]\|_{\text{HS}}^2 = |J_3(J_x - J_y)|^2/2 + 8|h_x(J_y - J_z)|^2$, where $\|X\|_{\text{HS}} = (\sum_{i,j=1}^m |X_{ij}|^2)^{1/2}$ is the Hilbert-Schmidt (HS) norm of an m-dimensional matrix X. Therefore, choosing $J := J_x = J_y = J_z$ (i.e., the Heisenberg XXX model), commutativity between H_T and H_{QS} is granted. By tuning J (see that J_3 and h_x are fixed) and comparing the eigenvalues of the resulting H_{QS} with those of H_T, it is possible to create degeneracy in the connector. The evolution under H_T of any initial state belonging to the subspace where the connector is degenerate can thus be exactly reproduced by the engineered H_{QS}. A particular example is displayed in Appendix A 1. Clearly, the same approach can also be taken for higher spatial dimensional systems, where spins have a larger number of next neighbors and thus exhibit a greater richness of interactions. However, since this approach requires diagonalization, implementing it in large systems is not viable. As a more systematic way, we introduce a method to search for the best simulator Hamiltonian in any dimension and with fixed locality in Proposition 2 by allowing for an error ϵ in the fidelity of simulation, and by restricting to the short-time regime.

B. Noncommuting Hamiltonians

Even if $[H_{QS}, H_T] \neq 0$, simulation is feasible in some cases. If both Hamiltonians share part of their eigenstates, it naturally follows from the previous approach that simulation can still be performed on the energy subspace spanned by those eigenstates. Let the set of shared eigenstates be $\Theta = \{|\varphi_j\rangle\}_{j=1}^{N_\Theta}$ (note that N_Θ depends on the basis on which each Hamiltonian is expressed) and let the projected connector be $h^{(\Theta)} := \sum_{i,j=1}^{N_\Theta} |\varphi_i\rangle\langle\varphi_i|h|\varphi_j\rangle\langle\varphi_j|$. Then the simulatable states $|\psi\rangle$ will be those living in the subspace where $h^{(\Theta)}$ is degenerate.

We illustrate with an example how two noncommuting Hamiltonians with different localities may generate the same dynamics in Appendix A 2. There again, we consider the H_T of the previous section as our 3-local target Hamiltonian. Our QS is now a (2-local) Heisenberg XXX model with 1-body terms,

$$\tilde{H}_{QS} = J \sum_{j=1}^{4} \left(\sigma_x^j \sigma_x^{j+1} + \sigma_y^j \sigma_y^{j+1} + \sigma_z^j \sigma_z^{j+1}\right) + b_x \sum_{j=1}^{4} \sigma_x^j + b_y \sum_{j=1}^{4} \sigma_y^j + b_z \sum_{j=1}^{4} \sigma_z^j, \tag{6}$$

where these 1-body terms prevent $\tilde{H}_{QS}$ from commuting with H_T.

Yet, a far more complex question is whether two given noncommuting high-dimensional Hamiltonians give rise to the same dynamics. The answer is generally negative, since the subset of Hamiltonians with only one common eigenstate is already of measure zero [18]. Moreover, computing the shared eigenstates entails diagonalizing such large Hamiltonians, which costs computational resources. Below, we derive an upper bound to the maximum number of such shared eigenstates, the calculation of which does not require diagonalization or computationally demanding techniques:

Lemma 1. The maximum number r of shared eigenstates of two N-dimensional noncommuting Hamiltonians H_T and H_{QS} is bounded as

$$r \leqslant N - \left(\frac{\|[H_T, H_{QS}]\|_{\text{HS}}}{\|[H_T, H_{QS}]\|_2}\right)^2, \tag{7}$$

where $\|X\|_2 = \max_{\|\mathbf{v}\|=1}(\|X\mathbf{v}\|)$ is the spectral norm of an n-dimensional matrix X, with $\mathbf{v}$ an n-dimensional vector and $\|\mathbf{v}\| = (\sum_{i=1}^n |\mathbf{v}_i|^2)^{1/2}$.

Proof. Consider two arbitrary N-dimensional square matrices $A_\mathcal{X}$ and $B_\mathcal{X}$, where $\mathcal{X}$ is the basis in which they are expressed. Their commutator can be written as $[A_\mathcal{X}, B_\mathcal{X}] = 0^{\oplus r_\mathcal{X}} \oplus C_\mathcal{X}$, with $r_\mathcal{X} \in \mathbb{N}$, $0^{\oplus p} := \underbrace{0 \oplus \ldots \oplus 0}_{p}$, and $C_\mathcal{X}$ some traceless $(N - r_\mathcal{X})$-dimensional matrix (without loss of generality, we have assumed that $A_\mathcal{X}$ and $B_\mathcal{X}$ share the first $r_\mathcal{X}$ eigenvectors). It then holds that $\|[A_\mathcal{X}, B_\mathcal{X}]\|_* = \|C_\mathcal{X}\|_*$, for any chosen matrix norm $*$. Let us consider the Hilbert-Schmidt norm, $\|\cdot\|_{\text{HS}}$, and the spectral norm, $\|\cdot\|_2$. Now, recall that $\|X\|_{\text{HS}} \leqslant \sqrt{m}\|X\|_2$, with $m = \dim X$ [19].

If matrix X is a finite-dimensional commutator (thus traceless), then the inequality can get saturated for even m if X is proportional to a diagonal matrix with half of their entries being 1, and half of them being -1. For n qubits (thus $m = 2^n$), the inequality is saturated when choosing $A_{\mathcal{X}} = ...\mathbb{1} \otimes \sigma_x \otimes \mathbb{1}...$ and $B_{\mathcal{X}} = ...\mathbb{1} \otimes \sigma_y \otimes \mathbb{1}....$ It then follows that $0 \leqslant \|[A_{\mathcal{X}}, B_{\mathcal{X}}]\|_{\mathrm{HS}} \leqslant \sqrt{N - r_{\mathcal{X}}}\|[A_{\mathcal{X}}, B_{\mathcal{X}}]\|_2$. Now, the maximum number of shared eigenvectors between $A_{\mathcal{X}}$ and $B_{\mathcal{X}}$ is given by

$$r := \max_{\mathcal{X}} r_{\mathcal{X}} \leqslant N - \left(\frac{\|[A_{\mathcal{X}}, B_{\mathcal{X}}]\|_{\mathrm{HS}}}{\|[A_{\mathcal{X}}, B_{\mathcal{X}}]\|_2}\right)^2, \tag{8}$$

since the considered norms are unitarily invariant. This completes the proof. ■

Note that the calculation of the spectral norm is efficient as it is expressible by a semidefinite program [20]. This upper bound, which is tight for even dimension N, informs about the maximal size that the shared subspace could have, helping to decide whether it is still worth trying to search for the shared eigenstates even by using diagonalization. Moreover, computing the upper bound to r can aid in the processes of figuring out the parameters of the corresponding H_{QS}. Suppose one can only prepare initial states $|\psi\rangle \in \mathcal{S} \subseteq \mathcal{H}_N$, where $\dim \mathcal{S} \leqslant N$. Recall that exact simulation is granted in a subspace of at least dimension $\dim \mathcal{S}^{(\Theta)}$, where $\mathcal{S}^{(\Theta)}$ is the subspace in which $h^{(\Theta)}$ is degenerate. Hence, $\dim \mathcal{S}^{(\Theta)} \leqslant r \leqslant N - \left(\frac{\|[H_T, H_{QS}]\|_{\mathrm{HS}}}{\|[H_T, H_{QS}]\|_2}\right)^2$. In order for the dynamics to be simulatable in this case, it is required that $\dim \mathcal{S} \leqslant \dim \mathcal{S}^{(\Theta)}$. If the current choice of the parameters of H_{QS} leads to $N - \left(\frac{\|[H_T, H_{QS}]\|_{\mathrm{HS}}}{\|[H_T, H_{QS}]\|_2}\right)^2 < \dim \mathcal{S}$, it holds that $\dim \mathcal{S} > \dim \mathcal{S}^{(\Theta)}$ and therefore one must search for a different set of parameters.

In addition, we prove a necessary condition for a state to be an eigenstate of two Hamiltonians with different localities and leave its derivation in Appendix D.

IV. APPROXIMATE SIMULATION

We now focus on the realistic scenario of approximate quantum simulation, i.e., the case when H_{QS} simulates H_T up to some tolerable error $\epsilon \neq 0$. Contrary to the setting with $\epsilon = 0$, looking at condition (1) does not reveal in a straightforward way how both Hamiltonians should be related in order for one to ϵ-simulate the other. Nonetheless, we are able to provide an upper bound to the error up to which such a simulation can be performed:

Theorem 1. [21] Every Hamiltonian H_{QS} ϵ^*-simulates any target Hamiltonian H_T at any state $|\psi\rangle$ and time t, with

$$\epsilon^* = \min\left[1, \frac{t\Delta_h}{2}\right]. \tag{9}$$

Here, Δ_h is the spectral diameter of the connector, $h := H_{QS} - H_T$, i.e., $\Delta_h = \max_{ij} |\lambda_i - \lambda_j|$, where $\{\lambda_i\}_{i=1}^N$ are the eigenvalues of h.

Proof. First note that $|\langle\psi|e^{itH_{QS}}e^{-itH_T}|\psi\rangle| = |\langle\psi|e^{it\tilde{H}_{QS}}e^{-itH_T}|\psi\rangle|$, with $\tilde{H}_{QS} = H_{QS} + c\mathbb{1}$, $c \in \mathbb{R}$. Now, it is well established that

$$1 - |\langle\psi|e^{it\tilde{H}_{QS}}\ e^{-itH_T}\ |\psi\rangle| \tag{10}$$

$$\begin{aligned}
&\leqslant |1 - \langle\psi|e^{it\tilde{H}_{QS}}e^{-itH_T}|\psi\rangle| \\
&= \left|\langle\psi|\int_t^0 ds\left(\frac{d}{ds}e^{is\tilde{H}_{QS}}e^{-isH_T}\right)|\psi\rangle\right| \\
&\leqslant \left|\int_t^0 ds\left\|\tilde{H}_{QS} - H_T\right\|_2\right| = t\left\|\tilde{H}_{QS} - H_T\right\|_2 = t\|h + c\mathbb{1}\|_2.
\end{aligned} \tag{11}$$

Therefore,

$$|\langle\psi|e^{itH_{QS}}e^{-itH_T}|\psi\rangle| \geqslant 1 - t\min_c \|h + c\mathbb{1}\|_2 = 1 - t\frac{\Delta_h}{2}, \tag{12}$$

and the proof is finished. ■

From here we see that the worst-case fidelity of simulation is never smaller than $1 - \epsilon^*$. We emphasize that the calculation of the error ϵ^* does not require diagonalization. The spectral diameter Δ_h is the difference between the largest and the smallest eigenvalue of h and can be obtained by means of a semidefinite program, as discussed later. As shown in Appendix E, other valid bounds can be derived for the worst-case fidelity of simulation, but they are smaller than the proved $1 - \epsilon^*$.

Notice that $1 - \epsilon^*$ is greater than zero if and only if $t\Delta_h < 2$. In this regime, for fixed time t, we see that the smaller Δ_h, the higher $1 - \epsilon^*$. Now note that since H_{QS} is a k'-local Hamiltonian and H_T is a k-local Hamiltonian (with $k' < k$), h is a proper k-local Hamiltonian. One could ask at this point how the spectral diameter of a k-local Hamiltonian depends on k. To answer this open question, research in the direction of [22] would be required. They study the extremal eigenvalues of k-local Hamiltonians [with $k = \mathcal{O}(1)$] acting on n qubits, such that each qubit participates in at most l terms. Instead of showing, as they do, how such extremal eigenvalues change with the interaction l, one would need to examine how these vary with the locality k. A numerical route can be taken to explore such behaviors for particular cases. Here we ask what kind of H_{QS} yields the smallest spectral diameter Δ_h, when H_T is a Hamiltonian with k-body nearest-neighbor interactions in the z direction describing a one-dimensional array of qubits. For instance, for $k = 3$ we force the target to be $H_T = C_3 \sum_j \sigma_j^z \sigma_{j+1}^z \sigma_{j+2}^z$, where C_3 is just a normalization constant. As shown below, this problem can be cast as a semidefinite program:

Proposition 1. The following semidefinite program minimizes Δ_h when H_{QS} is k'-local and H_T is a k-local Hamiltonian with nearest neighbor interactions in the z direction describing a one-dimensional array of n qubits:

$$\begin{aligned}
&\min\ \lambda_1 - \lambda_0 \quad \text{s.t. } \lambda_0 \preceq H_{QS} - H_T \preceq \lambda_1 \\
&\mathrm{tr}\left[H_{QS}\Lambda_i^{(j)}\right] = 0 \ \ \forall i \quad \text{and} \quad \forall j > k' \\
&\mathrm{tr}\left[H_{QS}\Lambda_i^{(k')}\right] \geqslant \beta \ \ \forall i\ H_T = C_k \sum_{l=1}^{n} \sigma_l^z \ldots \sigma_{l+k-1}^z,
\end{aligned} \tag{13}$$

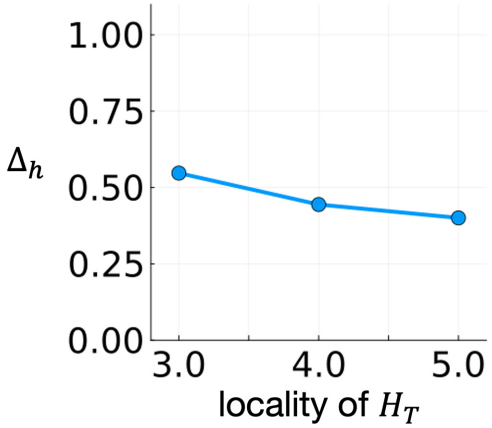

FIG. 1. Spectral diameter Δ_h minimised by the SDP (13) as a function of the locality of H_T.

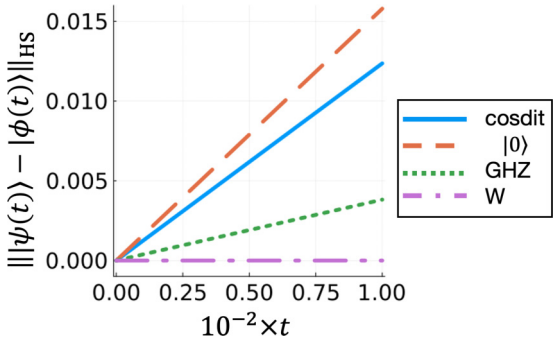

FIG. 2. Minimum HS norm between states $|\psi(t)\rangle = e^{-itH_T}|\psi_0\rangle$ and $|\phi(t)\rangle = e^{-itH_{QS}}|\psi_0\rangle$, where $|\psi_0\rangle$ are different initial states (a cosdit $\frac{1}{\sqrt{8}}\sum_{i=1}^{8}|i\rangle$, the $|0\rangle$ state, the GHZ state and the W state), H_T is a random 3-qubit 3-local Hamiltonian in 1D, and H_{QS} is a 3-qubit 2-local Hamiltonian in 1D.

where C_k is a normalization constant, $\Lambda_i^{(j)}$ are the generators of all possible j-body interactions, and $\beta \neq 0$ is the strength of the k'-body interactions of H_{QS}.

Note that the second constraint prevents H_{QS} from having local terms with localities larger than k'. Also, the third constraint forces H_{QS} to present nonvanishing k'-body interactions. Figure 1 shows the minimal spectral diameter Δ_h when H_T is a Hamiltonian with k-body nearest-neighbor interactions ($k = 3, 4, 5$) describing an array of five qubits, and H_{QS} has only 2-local interactions of strength larger than or equal to $\beta = 0.01$. Periodic boundary conditions are enforced on H_T. The minimal value of Δ_h decreases when H_T is less local, suggesting that such kind of target Hamiltonians are simulated to a better precision the less local they are.

Fixing now Δ_h in $t\Delta_h < 2$, simulators are expectedly more precise when restricting to short times. Here, we provide a program to find the k'-local Hamiltonian H_{QS} that best simulates a target k-local Hamiltonian H_T at a given state $|\psi\rangle$ for short times [in the precise sense that terms in $\mathcal{O}(t^2)$ are negligible]:

Proposition 2. The following program yields the minimum HS norm between states $|\psi(t)\rangle = e^{-itH_T}|\psi_0\rangle$ and $|\phi(t)\rangle = e^{-itH_{QS}}|\psi_0\rangle$ for state $|\psi_0\rangle$ and time $t \ll 1$, where H_T is a given k-local Hamiltonian and H_{QS}—the optimization variable—is k'-local:

$$\begin{aligned} &\min \|(\mathbb{1} - itH_T)|\psi_0\rangle - (\mathbb{1} - itH_{QS})|\psi_0\rangle\|_{\mathrm{HS}} \\ &\text{s.t. } \mathrm{Tr}\big(H_{QS}\,\Lambda_i^{(j)}\big) = 0 \quad \forall i, \end{aligned} \tag{14}$$

where $\Lambda_i^{(j)}$ are the generators of all possible j-body interactions, with $j > k'$.

Notice that the states $(\mathbb{1} - itH_X)|\psi_0\rangle$ are not normalized. It is possible to find a solution for this conic program using state-of-the-art solvers like [23]. In Fig. 2 we show the minimum HS norm between states $|\psi(t)\rangle = e^{-itH_T}|\psi_0\rangle$ and $|\phi(t)\rangle = e^{-itH_{QS}}|\psi_0\rangle$, for several paradigmatic initial states $|\psi_0\rangle$. Here, H_T is a random 3-qubit 3-local Hamiltonian in 1D, and H_{QS} is a 3-qubit 2-local Hamiltonian in 1D. The evolution of the W state can be reproduced exactly in this case. For the rest of the initial states, the plotted distance scales linearly with time in this short time regime.

V. DISCUSSION

We have explored the dynamic simulation of k-local Hamiltonians using more local Hamiltonians acting on the same Hilbert space, an approach that aligns effectively with the present experimental limitations: as argued in the Introduction, scaling up simulation platforms to accommodate remarkably larger simulator Hamiltonians is still a challenging task. In the exact simulation scenario, we have confirmed that some Hamiltonians with different localities can produce the same dynamics at certain subsets of states even if they do not commute. Further, we have analyzed the more realistic scenario where the dynamics is reproduced up to some error and provided a lower bound to the worst-case fidelity with which any Hamiltonian can simulate another one. Based on this, we have numerically shown evidence that the spectral diameter decreases as the locality increases, and this suggests that the simulation can be performed more precisely. Moreover, we have presented a program to find the Hamiltonian that best simulates a given k-local Hamiltonian in the short-time regime and solved it for a particular physical scenario.

The relation between the worst-case fidelity of simulation and the spectral diameter of the corresponding connector has been unveiled. This has allowed us to study dynamic simulatability without requiring diagonalization, which becomes computationally expensive when considering large systems. In turn, the relation between locality and spectral diameter needs to be further investigated in the line of [22], which would help us understand how to better engineer quantum simulation settings. Also, further research could be conducted in the spirit of [18] to calculate the relative volume of the simulatable sets of states, which would shed light on the potential of simulatability of each particular scenario.

ACKNOWLEDGMENTS

Discussions with Álvaro M. Alhambra and Tamara Kohler and comments from the referees are gratefully appreciated. A.U. is financially supported by Maria de Maeztu project (Grant No. CEX2019-000918-M funded by MCIN/AEI/10.13039/501100011033). M.G.D. was supported by Grant No. PID2020-113523GB-I00, funded by

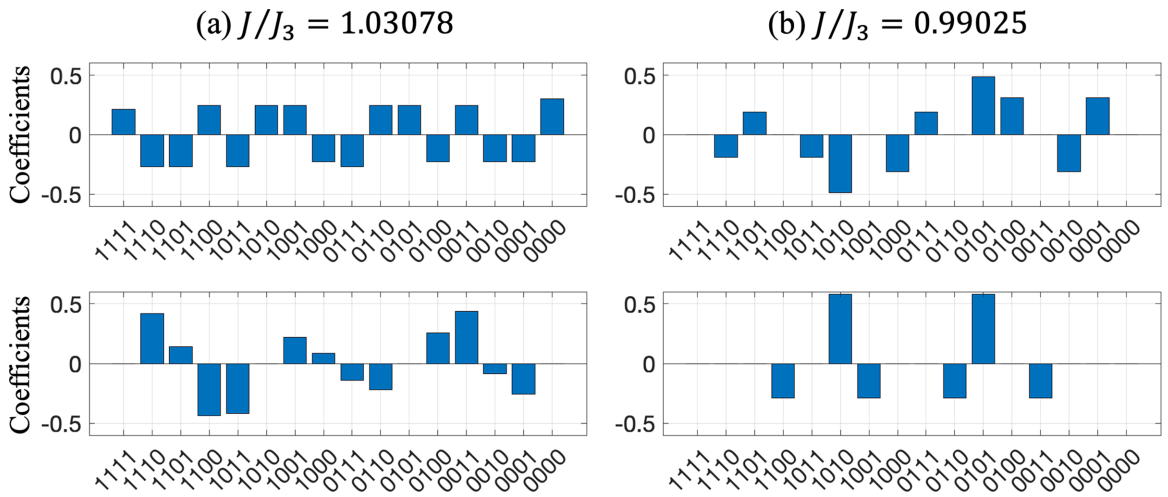

FIG. 3. Coefficients of two degenerate eigenstates of h and value of the parameter J/J_3. The x label denotes the spin basis, where "0" means spin down and "1" means spin up.

MCIN/AEI/10.13039/501100011033. We acknowledge support from the Spanish Agencia Estatal de Investigación and the Ministerio de Ciencia e Innovación (Grants No. PID2019-107609GB-I00 and No. PID2022-141283NB-I00). A.S. also acknowledges financial support from the European Commission QuantERA Grant ExTRaQT (Spanish MICINN Project No. PCI2022-132965), from the Spanish Ministry of Economic Affairs and Digital Transformation QUANTUM ENIA project call-Quantum Spain project, and by the European Union through the Recovery, Transformation and Resilience Plan-NextGenerationEU within the framework of the "Digital Spain 2026 Agenda", and by the Spanish MICINN with funding from European Union NextGenerationEU (PRTRC17.I1) and the Generalitat de Catalunya.

APPENDIX A: ILLUSTRATION OF EXACT SIMULATION WITH A HAMILTONIAN THAT IS DIFFERENT FROM THE TARGET ONE

We aim at showing two examples of Hamiltonians with different localities, which generate the same dynamics. We consider Eq. (4) as the target Hamiltonian and two different simulator Hamiltonians as discussed below.

1. Example 1: A simulator that commutes with H_T

As a simulator, we have considered the XXX model,

$$H_{QS} = J \sum_{j=1}^{4} \left(\sigma_x^j \sigma_x^{j+1} + \sigma_y^j \sigma_y^{j+1} + \sigma_z^j \sigma_z^{j+1}\right), \tag{A1}$$

which commutes with H_T for any J, J_3, and h_x, as mentioned in the main text. We take J_3 as the energy unit and here fix $h_x/J_3 = 1$, although this ratio can take any real value. We tune J/J_3 such that $h = H_{QS} - H_T$ has some degeneracy.

In terms of how to find the shared eigenvectors, we refer to Appendix B. We define the eigenvalues and the eigenvectors of H_T as $\{\lambda_j^T\}_j$ and $\{\phi_j^T\}_j$, and the eigenvectors $\{\phi_j^T\}_j$ are tailored to diagonalize H_{QS} as well. The eigenvalues $\{\lambda_j^{QS}\}_j$ of H_{QS} are linearly dependent on J, and, by denoting the eigenvalues of H_{QS} for $J/J_3 = 1$ with $\{\tilde{\lambda}_j^{QS}\}_j$, we have $\{\lambda_j^{QS}\}_j = J\{\tilde{\lambda}_j^{QS}\}_j$. By comparing $\{\lambda_j^{QS}\}_j$ and $\{\lambda_j^T\}_j$ and changing J, one can create some degeneracy in h.

We here show a few cases where h has two degenerate eigenstates. Figure 3 displays the parameter J/J_3 and the degenerate eigenstates of h of such cases. The same dynamics is generated by H_T and by H_{QS} as long as the initial state is spanned by such eigenstates.

2. Example 2: A simulator that does not commute with H_T

Consider a simulator $\tilde{H}_{QS}$ that does not commute with H_T, i.e., they may share only part of their eigenvectors. Our simulator is now a 2-local Heisenberg XXX model with 1-body terms,

$$\tilde{H}_{QS} = J \sum_{j=1}^{4} \left(\sigma_x^j \sigma_x^{j+1} + \sigma_y^j \sigma_y^{j+1} + \sigma_z^j \sigma_z^{j+1}\right) + b_x \sum_{j=1}^{4} \sigma_x^j + b_y \sum_{j=1}^{4} \sigma_y^j + b_z \sum_{j=1}^{4} \sigma_z^j, \tag{A2}$$

where these 1-body terms prevent $\tilde{H}_{QS}$ from commuting with H_T. Again, we take J_3 as the energy unit.

First, we search for the shared subspace. We refer the details to Appendix C, but note that the size of the shared subspace corresponds to the nullity of the commutator, i.e., the number of vanishing eigenvalues of the commutator. We choose the parameter set $\{b_x, b_y, b_z\}$ such that the nullity is large, while J is not involved in the eigenvalues of the commutator due to the fact that $[H_{QS}, H_T] = 0$. Thus, we take $\{b_x/J_3, b_y/J_3, b_z/J_3\} = \{-4, 0, 1\}$ and in this case the number of shared eigenstates is 12. The set of the shared eigenstates is obtained by constructing a proper linear combination of the eigenstates of the commutator (see Appendices B and C).

The only thing left is to create degeneracy in $\tilde{h} = H_{QS} - \tilde{H}_T$ in the corresponding subspace as we do in Appendix A 1. By tuning J, we have created some degeneracy in $\tilde{h}$. Figure 4

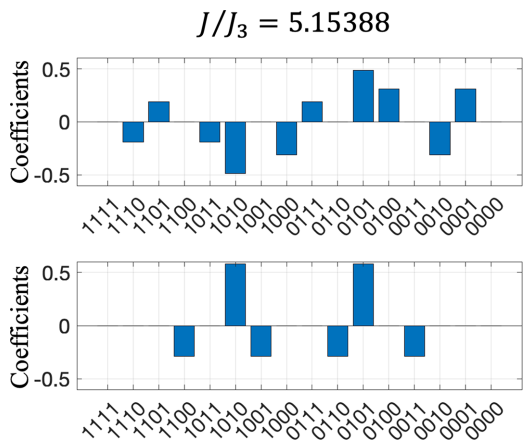

FIG. 4. Coefficients of two eigenstates degenerate in $\tilde{h}$ and the value of parameter J/J_3. The x label denotes the spin basis, where "0" means down spin and "1" means up spin.

displays the parameter J/J_3 and the degenerate eigenstates of $\tilde{h}$ of such cases.

APPENDIX B: SHARED EIGENSTATES OF TWO COMMUTING HAMILTONIANS

Two commuting Hamiltonians share all of their eigenstates. One can construct the shared eigenstates by using diagonalization, but there is an extra step to take if these Hamiltonians are both degenerate. Below, we explain how the shared eigenvectors of two commuting Hamiltonians are obtained. Our discussion is general but tailored for use in Appendix A.

Suppose two commuting Hamiltonians H_A and H_B. We consider two cases: (i) the case where the Hamiltonian H_A is not degenerate and (ii) the case where the Hamiltonian H_A has one set of degenerate eigenstates.

Let us start with case (i). We define $|\psi_n\rangle$ as the n-the eigenstate of H_A,

$$H_\mathrm{A}|\psi_n\rangle = a_n|\psi_n\rangle. \tag{B1}$$

We apply $H_\mathrm{A}H_\mathrm{B}$ on the state $|\psi_n\rangle$ and use $[H_\mathrm{A}, H_\mathrm{B}] = 0$,

$$H_\mathrm{A}H_\mathrm{B}|\psi_n\rangle = H_\mathrm{B}H_\mathrm{A}|\psi_n\rangle = a_nH_\mathrm{B}|\psi_n\rangle. \tag{B2}$$

This means that, if $H_\mathrm{B}|\psi_n\rangle \neq 0$, $H_\mathrm{B}|\psi_n\rangle$ is an eigenstate of H_A. Since H_A is not degenerate, $|\psi_n\rangle$ is only one eigenstate having a_n as its eigenvalue. Thus, this eigenstate $H_\mathrm{B}|\psi_n\rangle$ is essentially the same state as $|\psi_n\rangle$, and they differ only by a constant. We call this constant b_n, and therefore,

$$H_\mathrm{B}|\psi_n\rangle = b_n|\psi_n\rangle. \tag{B3}$$

If $H_\mathrm{B}|\psi_n\rangle = 0$, we say that $|\psi_n\rangle$ is an eigenstate of H_B with its eigenvalue $b_n = 0$.

Next, we consider case (ii) where H_A has a set of degenerate eigenstates. We cannot follow the same process as in case (i) because, when we obtain Eq. (B3), we rely on the fact that all the eigenvalues are different. Suppose that the n-th eigenvalue a_n is g-fold degenerate. Let us define $|\psi_n^r\rangle$ for $r = 1, 2, \ldots, g$ as its g-fold degenerate eigenstates: $H_\mathrm{A}|\psi_n^r\rangle = a_n|\psi_n^r\rangle$. The set of $\{|\psi_n^r\rangle\}_r$ is chosen such that they are orthonormalized via the Gram-Schmidt process. The state $H_\mathrm{B}|\psi_n^r\rangle$ can be expanded in a set of the degenerate eigenstates $\{|\psi_n^r\rangle\}_r$ as

$$H_\mathrm{B}\big|\psi_n^r\big\rangle = \sum_{s=1}^{g} c_{r,s}\big|\psi_n^s\big\rangle \tag{B4}$$

with a set of coefficients $c_{r,s}$, which is given by $\langle\psi_n^s|H_\mathrm{B}|\psi_n^r\rangle$ because

$$\big\langle\psi_n^{r'}\big|H_\mathrm{B}\big|\psi_n^r\big\rangle = \sum_{s=1}^{g} c_{r,s}\big\langle\psi_n^{r'}\big|\psi_n^s\big\rangle. = c_{r,r'}. \tag{B5}$$

Consider superposition between the degenerate states, $\sum_{r=1}^{g} d_r|\psi_n^r\rangle$ with d_r coefficient. We apply H_B to this state,

$$H_\mathrm{B}\sum_{r=1}^{g} d_r\big|\psi_n^r\big\rangle = \sum_{r=1}^{g}\sum_{s=1}^{g} d_rc_{r,s}\big|\psi_n^s\big\rangle = \sum_{s=1}^{g}\left(\sum_{r=1}^{g} c_{r,s}d_r\right)\big|\psi_n^s\big\rangle. \tag{B6}$$

The state $\sum_{r=1}^{g} d_r|\psi_n^r\rangle$ is an eigenstate of H_B with its eigenvalue b_n if

$$\sum_{r=1}^{g} c_{r,s}d_r = b_nd_s. \tag{B7}$$

Considering all the elements, this can be represented in matrix form,

$$c\vec{d} = b_n\vec{d}. \tag{B8}$$

The set of b_n and $\{d_r\}_r$ that satisfy the above equation is given by the eigenvalues and the eigenvectors of matrix c, respectively. We define the eigenvalues as $b_n^{(k)}$ and the eigenvectors as $\{d_r^{(k)}\}_r$ for $k = 1, 2, \ldots, g$. Therefore, the eigenvector of H_B with eigenvalue $b_n^{(k)}$ is given by $\sum_{r=1}^{g} d_r^{(k)}|\psi_n^r\rangle$. Of course, the eigenvalue of H_A with eigenvector $\sum_{r=1}^{g} d_r^{(k)}|\psi_n^r\rangle$ is a_n.

The point here is that any linear combination of $|\psi_n^r\rangle$ for all r can diagonlize H_A but may not diagonlize H_B. Therefore, it is necessary to find a linear combination of $|\psi_n^r\rangle$ that is an eigenstate of H_B. If H_A has multiple sets of degenerate states, we take this procedure for each set.

Note that the degeneracy of H_B does not matter in this process. Thus, if it is known that H_A is degenerate but H_B is not, it is efficient to use the eigenvectors of H_B as the shared eigenvectors instead.

APPENDIX C: SHARED SUBSPACE OF TWO NONCOMMUTING HAMILTONIANS

Even two noncommuting Hamiltonians may share some of their eigenstates. We explain how to find such shared eigenvectors below, and our discussion is general but tailored for use in Appendix A 2. First, consider two noncommuting Hamiltonians $\hat{H}_\mathrm{A}$, $\hat{H}_\mathrm{B}$ and calculate the commutator,

$$[\hat{H}_\mathrm{A}, \hat{H}_\mathrm{B}] = C, \tag{C1}$$

where C is a traceless matrix. Denoting a set of eigenvectors of the commutator with $\{|\phi_j\rangle\}_j$, we can have

$$\sum_{j=1}^{N} |\phi_j\rangle\langle\phi_j|[\hat{H}_\mathrm{A}, \hat{H}_\mathrm{B}]|\phi_j\rangle\langle\phi_j| = 0^{\oplus r} \oplus \tilde{C} \tag{C2}$$

with N the system size, $r \geqslant 0$ some integer and $\tilde{C}$ a diagonal and traceless matrix. The subspace spanned by the first r eigenvectors $\{|\phi_j\rangle\}_{j=1,\ldots,r}$ is the shared subspace, where the commutator is zero.

The first r eigenvectors $\{|\phi_j\rangle\}_{j=1,\ldots,r}$ may not diagonalize $\hat{H}_\mathrm{A}$ and $\hat{H}_\mathrm{B}$ in the subspace. It is the same reason why the eigenvectors of commuting degenerate Hamiltonians may not diagonalize one of the Hamiltonians as mentioned in Appendix B, and essentially these eigenvectors $\{|\phi_j\rangle\}_{j=1,\ldots,r}$ are degenerate in the commutator. One can find a linear combination of $\{|\phi_j\rangle\}_{j=1,\ldots,r}$ that diagonalizes $\hat{H}_\mathrm{A}$ and $\hat{H}_\mathrm{B}$ in the subspace by following the procedure introduced in Appendix B.

APPENDIX D: NECESSARY CONDITION FOR A STATE TO BE AN EIGENSTATE OF BOTH A k-LOCAL AND A k'-LOCAL HAMILTONIAN

Consider the set of k-local Hamiltonians, with basis $\{\Lambda_i\}$ and $\Lambda_i \in \mathrm{Herm}(\mathcal{H})$. For a given state $|\psi\rangle$, the corresponding correlation matrix is defined as

$$M_{ij}^{(k,\psi)} = \frac{1}{2}\langle\psi|\{\Lambda_i, \Lambda_j\}|\psi\rangle - \langle\psi|\Lambda_i|\psi\rangle\langle\psi|\Lambda_j|\psi\rangle. \quad \text{(D1)}$$

If the kernel of $M^{(k,\psi)}$ is not empty, then there exists at least one k-local Hamiltonian that is parent to $|\psi\rangle$ [24]. Since $M^{(k,\psi)}$ is Hermitian, it will have a nonempty kernel if and only if $\det M^{(k,\psi)} = 0$.

Now, recall that the set $\{\Lambda_i\}$ contains the generators of every possible j-body interaction, with $j \leqslant k$. Therefore, it contains the generators of all k-body interactions and the generators of all k'-body interactions, with $k' < k$. This implies that $M^{(k,\psi)}$ is a block matrix of the form

$$M^{(k,\psi)} = \left(\begin{array}{c|c} \mathcal{M}_{kk} & \mathcal{M}_{kk'} \\ \hline \mathcal{M}_{k'k} & \mathcal{M}_{k'k'} \end{array}\right), \quad \text{(D2)}$$

where $\mathcal{M}_{kk'}$ encompasses the correlations between the generators of the k-body and the k'-body interactions. The following lemma holds:

Lemma 2. If a state $|\psi\rangle$ is an eigenstate of both a k-local (with nonvanishing k'-local terms) and a k'-local Hamiltonian ($k' < k$), then

$$\sum_{r=1}^{N-1}\sum_{\alpha,\beta}(-1)^{s(\alpha)+s(\beta)}\det A[\alpha|\beta]\det B(\alpha|\beta) = -\det B, \quad \text{(D3)}$$

where $A = \mathcal{M}_{k'k'}$, $B = -\mathcal{M}_{k'k}\mathcal{M}_{kk}^{-1}\mathcal{M}_{kk'}$, and $N = \dim A = \dim B$. For a particular r, the inner sum is taken over all strictly increasing integer sequences α and β of length r, from 1 to N. $A[\alpha|\beta]$ is the r-square submatrix of A lying in rows α and columns β, $B(\alpha|\beta)$ is the $(N-r)$-square submatrix of B lying in rows complementary to α and columns complementary to β, and $s(\alpha)$ is the sum of the integers in α.

Proof. Since we do not want $|\psi\rangle$ to be an eigenstate only of a k-local Hamiltonian with vanishing k'-local terms, it is sound to assume that $\det \mathcal{M}_{kk} \neq 0$. Under this condition,

$$\det M^{(k,\psi)} = \det \mathcal{M}_{kk}\det\left(\mathcal{M}_{k'k'} - \mathcal{M}_{k'k}\mathcal{M}_{kk}^{-1}\mathcal{M}_{kk'}\right), \quad \text{(D4)}$$

which is zero when

$$\det\left(\mathcal{M}_{k'k'} - \mathcal{M}_{k'k}\mathcal{M}_{kk}^{-1}\mathcal{M}_{kk'}\right) = 0. \quad \text{(D5)}$$

Now recall that, for N-square matrices A and B [25],

$$\det(A+B) = \det A + \det B + \sum_{r=1}^{N-1}(-1)^{s(\alpha)+s(\beta)}\det A[\alpha|\beta] \times \det B(\alpha|\beta).$$

Define $A = \mathcal{M}_{k'k'}$ and $B = -\mathcal{M}_{k'k}\mathcal{M}_{kk}^{-1}\mathcal{M}_{kk'}$. If we want $|\psi\rangle$ to also be an eigenstate of a k'-local Hamiltonian, we must impose $\det A = 0$. Together with Eq. (D5), this yields

$$\sum_{r=1}^{N-1}\sum_{\alpha,\beta}(-1)^{s(\alpha)+s(\beta)}\det A[\alpha|\beta]\det B(\alpha|\beta) = -\det B,$$

and the proof is completed. ■

APPENDIX E: A WEAKER VERSION OF THEOREM 8

The following theorem can be derived:

Theorem 2. [21,26] Every Hamiltonian H_{QS} ϵ^*-simulates any target Hamiltonian H_T at any state $|\psi\rangle$ and time t, with

$$\epsilon^* = \min\left[1, \tfrac{1}{2}(e^{t\Delta_h} - 1), t\|h\|_{\mathrm{HS}}\right]. \quad \text{(E1)}$$

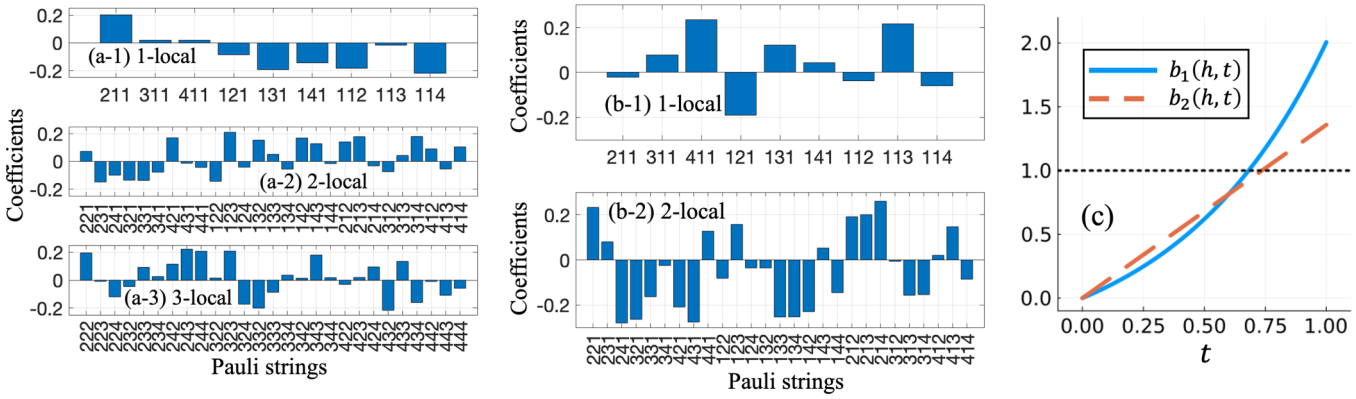

FIG. 5. (a) 3-qubit H_T, (b) 3-qubit H_{QS} and (c) behavior of the corresponding quantities $b_1(h,t)$ and $b_2(h,t)$. If the Hamiltonian is expressed as $H = \sum_l c_l P_l$, with $P_l \in \{\mathbb{1}, \sigma_x, \sigma_y, \sigma_z\}^{\otimes 3}$ a Pauli string, the x axis represents the Pauli strings $ijk \equiv P_l$, with $1 \equiv \mathbb{1}$, $2 \equiv \sigma_x$, $3 \equiv \sigma_y$, and $4 \equiv \sigma_z$. The corresponding coefficients, c_l, are shown in the y axis.

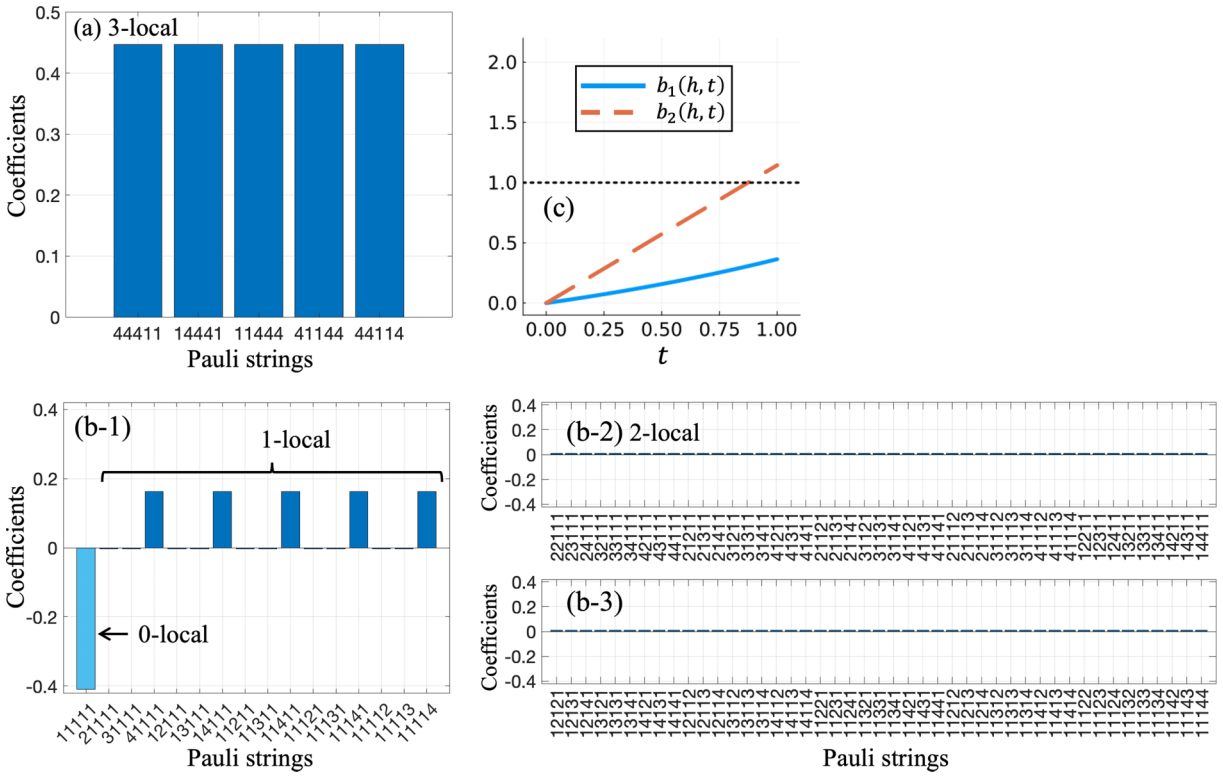

FIG. 6. (a) 5-qubit H_T, (b) 5-qubit H_{QS} and (c) behavior of the corresponding quantities $b_1(h,t)$ and $b_2(h,t)$. If the Hamiltonian is expressed as $H = \sum_l c_l P_l$, with $P_l \in \{\mathbb{1}, \sigma_x, \sigma_y, \sigma_z\}^{\otimes 5}$ a Pauli string, the x axis represents the Pauli strings $ijk \equiv P_l$, with $1 \equiv \mathbb{1}$, $2 \equiv \sigma_x$, $3 \equiv \sigma_y$, and $4 \equiv \sigma_z$. The corresponding coefficients, c_l, are shown in the y axis.

Here, Δ_h is the spectral diameter of the connector, $h := H_{QS} - H_T$, i.e., $\Delta_h = \max_{ij} |\lambda_i - \lambda_j|$, where $\{\lambda_i\}_{i=1}^N$ are the eigenvalues of h.

Proof. The bound $\epsilon^* = \min[1, \frac{1}{2}(e^{t\Delta_h} - 1)]$ is based on a beautiful result derived in [26]. There, the authors show that the trace distance between two states evolved under different time-dependent Hamiltonians, $\Omega(t)$ and $\Omega^0(t)$, fulfills $D[\rho(t), \rho^0(t)] \leqslant \min[1, \frac{1}{2}(e^{t\Delta\lambda(t)} - 1)]$, where $\rho(t) = e^{-it[\Omega(t),\cdot]}\rho(0)$, $\rho^0(t) = e^{-it[\Omega^0(t),\cdot]}\rho(0)$, and $\Delta\lambda(t)$ is the spectral diameter of $\Omega(t) - \Omega^0(t)$. The derivation is completed by applying that the fidelity between two pure states, $F(|\psi\rangle, |\phi\rangle) = |\langle\psi|\phi\rangle|$, is lower bounded as $F(|\psi\rangle, |\phi\rangle) \geqslant 1 - D(|\psi\rangle\langle\psi|, |\phi\rangle\langle\phi|)$, with $D(\sigma, \tilde{\sigma}) = \frac{1}{2}\mathrm{tr}|\sigma - \tilde{\sigma}|$.

We now proceed to derive $\epsilon^* = \min[1, t\|h\|_{\mathrm{HS}}]$ [21]. First, we have that

$$D(e^{-itH_T}|\psi\rangle\langle\psi|e^{itH_T}, e^{-itH_{QS}}|\psi\rangle\langle\psi|e^{itH_{QS}}) \overset{(a)}{\leqslant} \left\|(e^{-itH_T} - e^{-itH_{QS}})|\psi\rangle\right\|_2 \overset{(b)}{\leqslant} \left\|e^{-itH_T} - e^{-itH_{QS}}\right\|_{\mathrm{HS}} \overset{(c)}{\leqslant} t\|h\|_{\mathrm{HS}}.$$

Let us give the details of each inequality. In (a) we have used that, for pure states $|\psi\rangle$ and $|\phi\rangle$, it holds that $D(|\psi\rangle\langle\psi|, |\phi\rangle\langle\phi|) \leqslant \||\psi\rangle - |\phi\rangle\|_2$, where $\|\cdot\|_2$ is the Euclidean norm of a vector. In (b) we have employed the Cauchy-Schwarz inequality and the fact that $|\psi\rangle$ is normalized. In (c) we have first applied the triangle inequality to a telescoping sum. For $A := -itH_T$ and $B := -itH_{QS}$ we get

$$\begin{aligned}\left\|e^A - e^B\right\|_{\mathrm{HS}} &= \left\|\sum_{k=1}^m e^{(k-1)A/m}(e^{A/m} - e^{B/m})e^{(m-k)B/m}\right\|_{\mathrm{HS}} \\ &\leqslant \sum_{k=1}^m \|e^{(k-1)A/m}(e^{A/m} - e^{B/m})e^{(m-k)B/m}\|_{\mathrm{HS}} \\ &= m\|e^{A/m} - e^{B/m}\|_{\mathrm{HS}}, \end{aligned} \tag{E2}$$

for any $m \in \mathbb{N}$. Note that the last equality holds since the HS norm is unitarily invariant. Finally, expanding $e^{A/m}$ and $e^{B/m}$ into power series and letting $m \to \infty$ immediately leads to $\|e^A - e^B\|_{\mathrm{HS}} \leqslant \|A - B\|_{\mathrm{HS}}$. Apply $F(|\psi\rangle, |\phi\rangle) \geqslant 1 - D(|\psi\rangle\langle\psi|, |\phi\rangle\langle\phi|)$ and the proof is finished. ■

Notice that this theorem is weaker than Theorem 2, since $\frac{1}{2}(e^{t\Delta_h} - 1) \geqslant \frac{t\Delta_h}{2}$, and $\|h\|_{\mathrm{HS}} \geqslant \|h\|_2$.

What is more, neither of the bounds, $b_1(h,t) := \frac{1}{2}(e^{t\Delta_h} - 1)$ nor $b_2(h,t) := t\|h\|_{\mathrm{HS}}$, can universally upper-bound the other. We hereby present two examples of connectors leading to different behaviors of $b_1(h,t)$ with respect to $b_2(h,t)$.

First, we consider the randomly generated 3-local target Hamiltonian and the 2-local QS Hamiltonian of Fig. 5. As shown in the figure, as long as $b_1(h,t)$ and $b_2(h,t)$ are smaller than 1, $b_1(h,t)$ is smaller than $b_2(h,t)$ for times $t < 0.6$, and greater than it otherwise.

Secondly, we take the 3-local target Hamiltonian of Proposition 1 and a 2-local QS Hamiltonian (see Fig. 6). As shown in the figure, as long as $b_1(h,t)$ and $b_2(h,t)$ are smaller than 1, $b_1(h,t)$ is always smaller than $b_2(h,t)$.

[1] R. P. Feynman, Simulating physics with computers, Int. J. Theor. Phys. **21**, 467 (1982).

[2] E. Altman, K. R. Brown, G. Carleo, L. D. Carr, E. Demler, C. Chin, B. DeMarco, S. E. Economou, M. A. Eriksson, K.-M. C. Fu *et al.*, Quantum simulators: Architectures and opportunities, PRX Quantum **2**, 017003 (2021).

[3] M. Lewenstein, A. Sanpera, and V. Ahufinger, *Ultracold Atoms in Optical Lattices: Simulating Quantum Many Body Physics* (Oxford University Press, Oxford, 2012).

[4] I. M. Georgescu, S. Ashhab, and F. Nori, Quantum simulation, Rev. Mod. Phys. **86**, 153 (2014).

[5] J. I. Cirac and P. Zoller, Goals and opportunities in quantum simulation, Nat. Phys. **8**, 264 (2012).

[6] T. H. Johnson, S. R. Clark, and D. Jaksch, What is a quantum simulator? EPJ Quantum Technol. **1**, 10 (2014).

[7] S. Lloyd, Universal quantum simulators, Science **273**, 1073 (1996).

[8] Y. Subaşı and C. Jarzynski, Nonperturbative embedding for highly nonlocal Hamiltonians, Phys. Rev. A **94**, 012342 (2016).

[9] T. S. Cubitt, A. Montanaro, and S. Piddock, Universal quantum Hamiltonians, Proc. Natl. Acad. Sci. USA **115**, 9497 (2018).

[10] C. Mc Keever and M. Lubasch, Classically optimized Hamiltonian simulation, Phys. Rev. Res. **5**, 023146 (2023).

[11] T. Kohler, S. Piddock, J. Bausch, and T. Cubitt, Translationally invariant universal quantum Hamiltonians in 1D, Annales Henri Poincaré **23**, 223 (2022).

[12] T. Kohler, S. Piddock, J. Bausch, and T. Cubitt, General conditions for universality of quantum Hamiltonians, PRX Quantum **3**, 010308 (2022).

[13] L. Zhou and D. Aharonov, Strongly universal Hamiltonian simulators, arXiv:2102.02991.

[14] J. Kempe, A. Kitaev, and O. Regev, The complexity of the local hamiltonian problem, in *FSTTCS 2004: Foundations of Software Technology and Theoretical Computer Science*, edited by K. Lodaya and M. Mahajan (Springer, Berlin, 2005), pp. 372–383.

[15] K. Gietka, A. Usui, J. Deng, and T. Busch, Simulating the same physics with two distinct Hamiltonians, Phys. Rev. Lett. **126**, 160402 (2021).

[16] B. S. Mityagin (unpublished).

[17] S. Blanes and F. Casas, On the convergence and optimization of the Baker-Campbell-Hausdorff formula, Linear Algebra Appl. **378**, 135 (2004).

[18] M. G. Díaz, G. Sentís, R. M. Tapia, and A. Sanpera, Volumes of parent Hamiltonians for benchmarking quantum simulators, Phys. Rev. Res. **4**, 023228 (2022).

[19] R. Horn and C. Johnson, *Matrix Analysis* (Cambridge University Press, Cambridge, 2012).

[20] J. Watrous, Semidefinite programs for completely bounded norms, Theory Comput. **5**, 217 (2009).

[21] We thank the anonymous referee whose helpful comments led us to derive the bound proportional to the HS norm of the connector.

[22] A. W. Harrow and A. Montanaro, Extremal eigenvalues of local Hamiltonians, Quantum **1**, 6 (2017).

[23] MOSEK ApS, The MOSEK optimization toolbox for MATLAB manual. Version 10.0. (2022).

[24] X.-L. Qi and D. Ranard, Determining a local Hamiltonian from a single eigenstate, Quantum **3**, 159 (2019).

[25] M. Marcus, *Finite Dimensional Multilinear Algebra, Part II* (M. Dekker, New York, 1975), pp. 162–163.

[26] D. A. Lidar, P. Zanardi, and K. Khodjasteh, Distance bounds on quantum dynamics, Phys. Rev. A **78**, 012308 (2008).